

# Hamiltonian theory of fractionally filled Chern bands

Ganpathy Murthy<sup>1</sup> and R. Shankar<sup>2</sup>

<sup>1</sup> *Department of Physics and Astronomy, University of Kentucky, Lexington KY 40506-0055*

<sup>2</sup> *Department of Physics, Yale University, New Haven CT 06520*

(Dated: July 25, 2012)

There is convincing numerical evidence that fractional quantum Hall (FQH)-like ground states arise in fractionally filled Chern bands (FCB). Here we show that the Hamiltonian theory of Composite Fermions (CF) can be as useful in describing the FCB as it was in describing the FQHE in the continuum. We are able to introduce CFs into the FCB problem even though there is no external magnetic field by following a two-stage process. First we construct an algebraically exact mapping which expresses the electron density projected to the Chern band,  $\rho_{\text{FCB}}$ , as a sum of Girvin-MacDonald-Platzman density operators,  $\rho_{\text{GMP}}$ , that obey the Magnetic Translation Algebra. Next, following our Hamiltonian treatment of the FQH problem, we rewrite the GMP operators in terms of CF variables which reproduce the same algebra. This naturally produces a unique Hartree-Fock ground state for the CFs, which can be used as a springboard for computing gaps, response functions, temperature-dependent phenomena, and the influence of disorder. We give two concrete examples, one of which has no analog in the continuum FQHE with  $\nu = \frac{1}{5}$  and  $\sigma_{xy} = \frac{2}{5}$ . Our approach can be easily extended to fractionally filled, strongly interacting two-dimensional time-reversal-invariant topological insulators.

PACS numbers:

## I. INTRODUCTION AND STRATEGY

Models with no net magnetic flux but with a quantized Hall conductance  $\sigma_{xy}$  have been known since the work of Haldane<sup>1</sup> and Volovik<sup>2</sup>. The breaking of time-reversal symmetry, necessary for  $\sigma_{xy} \neq 0$ , manifests itself as a nontrivial Berry flux for the band, whose non-zero integral over the Brillouin zone (BZ) gives the Chern number  $\mathcal{C}$ . The work of Thouless *et al*<sup>3</sup>, equates  $\mathcal{C}$  to the dimensionless Hall conductance of the filled band. We use a convention in which  $\sigma_{xy} = -\mathcal{C}$ .

While we focus on single Chern bands, the approach to be described here readily applies to strongly interacting two dimensional time-reversal invariant topological insulators (2DTIs)<sup>4,5</sup> which can be thought of as pairs of time reversed Chern bands.

A question that has recently attracted much attention is whether these FCB's could also exhibit the FQHE at partial filling in the presence of suitable interactions. In such cases they are called fractional Chern insulators, or FCIs. Optimal conditions call for a hierarchy of scales, where the band gap  $\Delta$ , the interaction strength  $V_{ee}$ , and the FCB bandwidth  $W$  obey  $\Delta \gg V_{ee} \gg W$ . There have been three fronts of attack. Numerical efforts have concentrated on "flattening" the FCB<sup>6-8</sup>, and realized Laughlin-like states by exact diagonalization<sup>7-12</sup>. Most recently, other principal FQH fractions such as  $2/5$  and  $3/7$  have been seen as well<sup>13</sup>. On the analytical front, Qi<sup>14</sup> has constructed a basis in which known FQHE wavefunctions can be transcribed into the FCB. Recently Wu, Regnault and Bernevig<sup>15</sup> have pointed out that if Qi's plan is to yield wavefunctions with substantial overlap with the exact functions, his proposal must be modified to exploit a residual gauge freedom that maximizes the overlap. Several studies have likewise been devoted to the parton construction for FCIs<sup>16-18</sup> in which the electron is fractionalized into quarks, each of which is in an

Integer Quantum Hall state.

Our work was stimulated by the third approach due to Parameswaran *et al*<sup>19</sup> who examined the algebra of  $\rho_{\text{FCB}}(\mathbf{q})$ , the density operators projected into the FCB. Recall that in the LLL problem the projected density is essentially  $\rho_{\text{GMP}}(\mathbf{q})$ , the Girvin-MacDonald-Platzman<sup>20</sup> operator, which obeys the algebra of magnetic translations:

$$[\rho_{\text{GMP}}(\mathbf{q}), \rho_{\text{GMP}}(\mathbf{q}')] = 2i \sin \left[ \frac{l^2}{2} \mathbf{q} \times \mathbf{q}' \right] \rho_{\text{GMP}}(\mathbf{q} + \mathbf{q}'). \quad (1)$$

where

$$l = \frac{1}{\sqrt{eB_0}} \quad (2)$$

is the magnetic length associated with the perpendicular external field  $B_0$ . By contrast, the algebra of  $\rho_{\text{FCB}}(\mathbf{q})$  does not even close, though in the small  $\mathbf{q}, \mathbf{q}'$  limit the commutator is proportional to  $\mathbf{q} \times \mathbf{q}'$ . The fundamental reason for the non-closure of the density algebra is the varying Chern density  $\mathcal{B}(\mathbf{p})$  in the Brillouin Zone. Parameswaran *et al* offer interesting ways to combat the varying  $\mathcal{B}$ , such as smoothing it out or replacing it by its average.

Our approach, by contrast, tackles the varying Chern density from the outset. It is based on two indisputable facts:

- We are looking for the FQHE in the FCB problem.
- Composite Fermions are very useful in describing the FQHE problem in the continuum<sup>21</sup>.

It is then reasonable to ask if CFs can be made play an equally fruitful role in the FCB problem. Our answer is an emphatic yes. We employ the Hamiltonian

approach<sup>22</sup>, which provides an operator realization of CFs. In the past this has allowed us to compute not only gaps but also correlation functions at non-zero  $q, \omega$  and  $T$  and disorder. At  $\nu = \frac{1}{2}$  it yielded relaxation rates and polarization as a function of  $T$ . We describe how these ideas can be imported to the FCB problem.

The Hamiltonian theory of CFs presumes the existence of a uniform external magnetic field  $B_0$ . To those who say "Where did the magnetic field come from?", we say "Where did it go when the  $\nu = \frac{1}{2}$  state was described as a Fermi sea?"<sup>23</sup>. We adopt the pragmatic view that one must choose whichever mapping takes us closest to the desired end product. In the present case, when we want to describe FQH-like physics in a Chern band, LL-based constructs are a natural platform from which to make the leap. Furthermore, as shown by the recent work of Wu, Jain, and Sun<sup>24</sup>, the Hofstadter problem is adiabatically connected to the Chern band problem.

### A. Brief history of the Composite Fermion

Let us begin by asking what we mean by the CF, since the term has many connotations.

It all began with the realization that in two dimensions the statistics of particles could be altered by a singular gauge transformation of the wavefunctions that essentially attached flux tubes to the particles<sup>25</sup>. For fractions of the form  $\nu = \frac{1}{2s+1}$ , Zhang, Hansson and Kivelson<sup>26</sup> converted the electron to a composite boson by attaching  $2s+1$  flux quanta in the path-integral formulation of a Chern-Simons theory. They then explained many of the FQHE effects in terms of Bose condensation. Jain<sup>21</sup> then discovered that when  $\nu = \frac{p}{2ps+1}$ , one could get excellent trial wavefunctions by converting an electron to another (Composite) fermion by attaching  $2s$  flux quanta. Lopez and Fradkin<sup>27</sup> implemented this flux attachment for Jain fractions in a Chern-Simons path integral and computed response functions. These flux-attached CFs live in the full fermionic Hilbert space, have a bare mass, and carry the same charge as the electron, i.e.,  $e^* = e$ . They proved especially useful in the gapless state at  $\nu = \frac{1}{2}$ , analyzed in depth by Halperin, Lee and Read<sup>23</sup>.

The mean-field wavefunction due to *flux attachment* for fractions of the form  $\nu = \frac{p}{2p+1}$  is

$$\Psi^{CS} = \prod_{i < j} \frac{(z_i - z_j)^2}{|z_i - z_j|^2} \chi_p(z, \bar{z}) \quad (3)$$

where  $\chi_p$  stands for  $p$ -filled CF-LLs. Jain's ansatz

$$\Psi^{Jain} = \mathcal{P} \prod_{i < j} (z_i - z_j)^2 \chi_p(z, \bar{z}) \quad (4)$$

is obtained by dropping  $|z_i - z_j|^2$  and projecting the  $\bar{z}$  in  $\chi_p$  to the LLL using  $\mathcal{P} : \bar{z} \rightarrow 2l^2 \partial / \partial z$ . The double zero in the analytic Jastrow factor describes the charge deficit due to a double vortex that follows the electron,

leading to a CF that has  $e^* = e(1 - \frac{2p}{2p+1}) = \frac{e}{2p+1}$ . This is the CF obtained by *vortex attachment*.

In the path integral approaches<sup>26,27</sup> the change from flux attachment to vortex attachment is achieved by considering fluctuations about the mean-field, while in our earlier Hamiltonian approach<sup>28</sup> plasmon correlations *a la* Bohm-Pines were responsible.

### B. Brief review of the Hamiltonian theory

We work<sup>22</sup> with CFs that live in the LLL from the beginning, as did Read<sup>29</sup>, and Pasquier and Haldane<sup>30</sup>. Our CFs carry both the phase and charge deficit of a double zero in the FQHE wavefunction<sup>21,31</sup>. Their entire Hamiltonian is given by the electron-electron interaction projected to the LLL.

We introduce CFs as follows. The FQH problem projected to the LLL is defined by the Hamiltonian

$$\bar{H} = \frac{1}{2} \sum_{\mathbf{q}} \rho_{\text{LLL}}(\mathbf{q}) v_{ee}(\mathbf{q}) \rho_{\text{LLL}}(-\mathbf{q}) \quad (5)$$

where  $\rho_{\text{LLL}}(\mathbf{q})$  is the electron density projected to the LLL. In first quantization the full electron density is

$$\rho(\mathbf{q}) = \sum_j e^{i\mathbf{q} \cdot \mathbf{r}_e}. \quad (6)$$

The electron's position  $\mathbf{r}_e$  may be decomposed as

$$\mathbf{r}_e = \mathbf{R}_e + \boldsymbol{\eta}_e \quad (7)$$

where the electronic guiding center coordinate  $\mathbf{R}_e$  and cyclotron coordinate  $\boldsymbol{\eta}_e$  obey

$$[R_{ex}, R_{ey}] = -il^2 \quad (8)$$

$$[\eta_{ex}, \eta_{ey}] = il^2 \quad (9)$$

$$[\boldsymbol{\eta}_e, \mathbf{R}_e] = 0. \quad (10)$$

Upon projecting to the LLL

$$\rho_{\text{LLL}}(\mathbf{q}) = \sum_j \langle e^{i\mathbf{q} \cdot \boldsymbol{\eta}_{ej}} \rangle_{\text{LLL}} e^{i\mathbf{q} \cdot \mathbf{R}_{ej}} = e^{-q^2 l^2 / 4} \rho_{\text{GMP}}(\mathbf{q}). \quad (11)$$

where each term  $e^{i\mathbf{q} \cdot \mathbf{R}_{ej}}$  in the sum obeys the GMP algebra by itself thanks to Eq. 8. We shall use the same symbol for the densities when we switch to second quantization.

So the Hamiltonian to solve is

$$\bar{H} = \frac{1}{2} \sum_{\mathbf{q}} \rho_{\text{GMP}}(\mathbf{q}) \bar{v}_{ee}(\mathbf{q}) \rho_{\text{GMP}}(-\mathbf{q}) \quad (12)$$

where  $\bar{v}_{ee}(\mathbf{q}) = v_{ee}(\mathbf{q}) e^{-q^2 l^2 / 2}$ . The problem is difficult because, with  $\boldsymbol{\eta}_e$  projected to the LLL, the electron is described by just one canonical pair  $\mathbf{R}_e$  and not two. The LLL projected electron has half the degrees of freedom of

a regular two-dimensional fermion. However, the biggest problem is that at fractional filling there is no clear mean-field state.

We attack these problems as follows. First we introduce an auxiliary pair of conjugate "vortex" guiding center coordinates  $\mathbf{R}_v$ . They are defined by their commutation relations:

$$[R_{vx}, R_{vy}] = i \frac{l^2}{c^2} \quad (13)$$

$$c^2 = \frac{2p}{2p+1} \quad (14)$$

Evidently the vortex describes a particle whose charge  $-\frac{2p}{2p+1}$  in electronic units is exactly that of the two vortices in the Jastrow factor. It too has just half the degrees of freedom of a regular two-dimensional particle.

We want these auxiliary coordinates to commute with everything electronic i.e.,

$$[\mathbf{R}_e, \mathbf{R}_v] = 0. \quad (15)$$

*The cornerstone of our approach is that we can accommodate both  $\mathbf{R}_e$  and  $\mathbf{R}_v$  and their algebra very neatly into the Hilbert space of a regular two-dimensional fermion, which is going to be our composite fermion.* This fermion feels the reduced field  $B^*$  seen by a charge  $e^*$  object. In terms of its guiding center and cyclotron coordinates (which carry no subscripts like  $e$  or  $v$ ) that obey

$$[\eta_x, \eta_y] = i l^{*2} = i \frac{l^2}{1 - c^2} \quad (16)$$

$$[R_x, R_y] = -i l^{*2} \quad (17)$$

$$[\boldsymbol{\eta}, \mathbf{R}] = 0 \quad (18)$$

the algebra of the two conjugate pairs  $\mathbf{R}_e$  and  $\mathbf{R}_v$  can be realized as follows:

$$\mathbf{R}_e = \mathbf{R} + \boldsymbol{\eta} c \quad (19)$$

$$\mathbf{R}_v = \mathbf{R} + \boldsymbol{\eta}/c. \quad (20)$$

This in turn permits the crucial *CF substitution*

$$\rho_{\text{GMP}}(\mathbf{q}) = \sum_j \exp[i\mathbf{q} \cdot (\mathbf{R}_j + c\boldsymbol{\eta}_j)] \quad (21)$$

in Eqn. 12 for the projected Hamiltonian  $\bar{H}$ , which now acts on a regular fermionic Hilbert space with two conjugate pairs per particle. Since the CFs see exactly the right field to fill an integer number of CF-LLs, a natural, gapped Hartree-Fock state emerges. The price we pay for obtaining a good mean-field starting point is that our Hilbert space has unphysical degrees of freedom  $\mathbf{R}_v$ . In order to work in the physical sector the vortex coordinates need to be constrained. Specifically, the vortex densities,  $\rho_v(\mathbf{q}) = e^{i\mathbf{q} \cdot \mathbf{R}_v}$ , emerge as a gauge algebra. The way to handle this gauge degree of freedom is described in our review<sup>22</sup>.

The numbers computed in this scheme at nonzero  $\omega, q, T$  and disorder agree with data at the 10-15 % level<sup>22</sup>.

How is this formalism, predicated on making the CF-substitution in  $\rho_{\text{GMP}}$ , to be applied to the Chern band problem where the density of interest is  $\rho_{\text{FCB}}$ ? The key is to establish the following algebraically exact mapping:

$$\rho_{\text{FCB}}(\mathbf{q}) = \sum_{\mathbf{G}} c(\mathbf{G}, \mathbf{q}) \rho_{\text{GMP}}(\mathbf{q} + \mathbf{G}) \quad (22)$$

where the coefficients  $c(\mathbf{G}, \mathbf{q})$  can be computed from the data on the original Chern band, essentially by Fourier transformation. The CF-substitution can be then made in each  $\rho_{\text{GMP}}(\mathbf{q} + \mathbf{G})$ . While an explicit demonstration follows later, here is the gist of the argument. On an  $N \times N$  toroidal lattice the number of possible values for  $\mathbf{p}$  and  $\mathbf{q}$  are  $N^2$  each. We will show that the  $\rho_{\text{GMP}}(\mathbf{q} + \mathbf{G})$  are linearly independent only for  $N^2$  values of  $\mathbf{G}$  for each  $\mathbf{q}$  restricted to the Brillouin Zone (BZ). These  $N^4$  linearly independent operators  $\rho_{\text{GMP}}(\mathbf{q} + \mathbf{G})$  form a complete basis for one-body operators, just like the canonical basis  $d^\dagger(\mathbf{p}_i)d(\mathbf{p}_j)$  [ $i, j = 1 \dots N^2$ ].

The outline of the paper is as follows. In Section II we will show that our approach applies to a (Type I) Chern band with a variable Chern density  $\mathcal{B}(\mathbf{p})$  and coulomb interaction between electrons. This Chern band is obtained by starting with two electronic LLs and applying a periodic potential  $V_{\text{PP}}$  which mixes the LLs and causes  $\mathcal{B}(\mathbf{p})$  to vary. The lower band, the Modified Lowest Landau Level, or MLLL is our Chern band with  $\mathcal{C} = -1$ . We explicitly derive Eq. 22 (with the MLLL being the FCB), compute the coefficients  $c(\mathbf{G}, \mathbf{q})$  and calculate the band structure of CFs in the HF approximation.

In Section III we show how, given a *specific* lattice Chern band and an interaction between electrons, one can introduce CFs *without any reference to LLs*. We choose as our Type II example the Lattice Dirac Model (LDM):

$$H(\mathbf{p}) = \sigma_1 \sin p_x + \sigma_2 \sin p_y + \sigma_3 (M - \cos p_x - \cos p_y) \quad (23)$$

with  $M = 1$ , which lies in the regime with  $\mathcal{C} = -1$ .

Models in which LLs appear or do not appear explicitly are labeled as Class I and Class II respectively.

In Section IV we ask what happens if we apply our approach to a band with  $\mathcal{C} = 0$ , while in Section V we turn our attention to FQH-like states that owe their very existence to the lattice potential. Flux attachment on a lattice was first investigated in the context of anyonic states<sup>32,33</sup>, and analyzed in the FQH context by Kol and Read<sup>34</sup>. In such states, due to the explicit breaking of Galilean symmetry, the dimensionless Hall conductance need not be equal to the filling factor. There is suggestive numerical evidence of such states in a problem of hard-core bosons in an external magnetic field<sup>35,36</sup>. By virtue of our mapping of the FCB problems to LLL problems, such states should exist in FCBs as well. We define and solve an illustrative Class I model at  $\nu = \frac{1}{5}$  and demonstrate the existence of such a state where  $\nu = \frac{1}{5}$  and  $\sigma_{xy} = \frac{2}{5}$ .

Section VI presents conclusions and open questions.

## II. CLASS I MODELS

The goal of this section is to convince the reader that a nonconstant  $\mathcal{B}(\mathbf{p})$  is no impediment to the CF substitution, and to flesh out the key expansion Eq. 22. We begin with the construction of a nontrivial Chern band with a non-constant  $\mathcal{B}(\mathbf{p})$ .

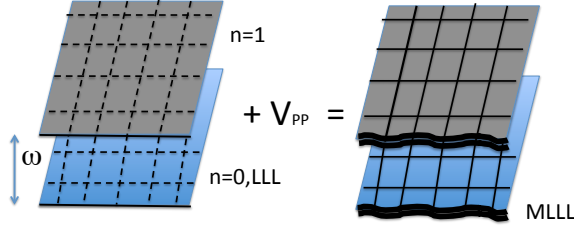


FIG. 1: Left: Two unperturbed Landau Levels with  $\mathcal{C} = -1$  and zero width separated by energy  $\omega$ . The dotted grid represents a fictitious square lattice with one flux quantum per unit cell. Right: The two bands with finite width after a periodic potential  $V_{PP}$  (solid grid) is imposed. The lower of the two bands, the Modified Landau Level, the MLLL, is our Chern band with  $\mathcal{C} = -1$ .

Consider a problem with two LLs labeled 0 and 1 separated by a gap  $\omega$  that is at our disposal, as shown in Fig.1. By choosing the Hamiltonian to be a suitable function of  $\eta_e^\dagger \eta_e$ , not simply linear, we can arrange for the other LLs to be separated by a parametrically larger gap than  $\omega$  and hence ignorable in what follows.

Each level has  $\mathcal{C} = -1$ . It is instructive to demonstrate this explicitly. (We recommend the review by Xiao, Chang and Niu for some basic ideas of magnetic Bloch bands<sup>37</sup>.) First we mentally superpose on this continuum immersed in a perpendicular field  $B_0$ , a square lattice of side  $a$ . No real periodic potential is applied yet. Working in the Landau gauge

$$A_y(x, y) = xB_0 \quad A_x(x, y) = 0 \quad (24)$$

we seek energy eigenfunctions which are also simultaneous eigenfunctions of  $T_x$  and  $T_y$ , the magnetic translation operators in the  $x$  and  $y$  directions:

$$T_x = e^{-iay_e l^{-2}} e^{a\partial_x} \quad T_y = e^{a\partial_y}. \quad (25)$$

These commute with  $H$ , but not with each other unless each unit cell has an integer number of flux quanta. We choose the simplest case of one flux quantum penetrating each unit cell, i.e.,

$$a^2 = 2\pi l^2. \quad (26)$$

The simultaneous eigenfunctions we seek are<sup>3</sup>:

$$\langle x_e, y_e | \mathbf{p}, n \rangle = \Psi_{\mathbf{p}, n}(x_e, y_e) \quad (27)$$

$$= \frac{1}{\sqrt{a}} \sum_{j=-\infty}^{\infty} e^{iy_e(p_y + ajl^{-2})} e^{iap_x j} \phi_n(x_e - aj - p_y l^2) \quad (28)$$

where  $\phi_n(x_e - aj - p_y l^2)$  is the wavefunction for an oscillator in level  $n$  centered at  $x_e = aj + l^2 p_y$ .

Hereafter we will set  $a = 1$  which means

$$l^2 = \frac{1}{2\pi}. \quad (29)$$

The states are normalized to unity, and  $\mathbf{r}_e$  integrals go over the unit cell.

The Bloch functions are

$$|u(\mathbf{p}, n)\rangle = e^{-i\mathbf{p} \cdot \mathbf{r}_e} |\mathbf{p}, n\rangle \quad (30)$$

and the Berry connection

$$\mathcal{A}(\mathbf{p}, n) = i\langle u(\mathbf{p}, n) | \nabla_{\mathbf{p}} | u(\mathbf{p}, n) \rangle \quad (31)$$

can be computed to have components

$$\mathcal{A}_y = 0 \quad \mathcal{A}_x = p_y l^2 = \frac{1}{2\pi} p_y \quad \text{so that} \quad (32)$$

$$\mathcal{B}(\mathbf{p}) = \nabla_{\mathbf{p}} \times \mathcal{A} = -\frac{1}{2\pi} \quad \text{which means} \quad (33)$$

$$\mathcal{C} = \frac{1}{2\pi} \int_{BZ} \mathcal{B} = -1. \quad (34)$$

However this  $\mathcal{B}$  is constant in  $\mathbf{p}$  in both LLs. To make it vary, we add a periodic potential

$$V(\mathbf{r}_e) = \sum_{\mathbf{G}} V(\mathbf{G}) e^{i\mathbf{G} \cdot \mathbf{r}_e} \quad (35)$$

which mixes the LLs and induces structure in  $\mathcal{B}(\mathbf{p})$ . In our illustrative example we keep only the harmonics  $\pm 2\pi$  in the two directions with coefficient  $V_{10}$ , though the following analysis applies to the general case. Using

$$\langle \mathbf{p} n_2 | e^{i\mathbf{G} \cdot \mathbf{r}} | \mathbf{p} n_1 \rangle = \rho_{n_2 n_1} e^{iG_x G_y / 4\pi} e^{i\mathbf{G} \times \mathbf{p} / 2\pi} \quad (36)$$

where (for the general value of  $l$ ),

$$\begin{aligned} \rho_{n_2 n_1}(\mathbf{q}) &= e^{-q^2 l^2 / 4} \sqrt{\frac{n_{<}!}{n_{>}!}} L_{n_{<}}^{|n_1 - n_2|} \left[ \frac{q^2 l^2}{2} \right] \\ &\times \begin{cases} \left( \frac{il\bar{z}}{\sqrt{2}} \right)^{|n_1 - n_2|} & \text{when } n_1 > n_2 \\ \left( \frac{ilz}{\sqrt{2}} \right)^{|n_1 - n_2|} & \text{when } n_2 \geq n_1 \end{cases} \\ z &= q_x + iq_y \end{aligned} \quad (37)$$

we find

$$H^I(\mathbf{p}) = \left[ g(\mathbf{p}) - \tilde{V}\sigma_1 \sin p_y + \tilde{V}\sigma_2 \sin p_x \right. \\ \left. - \sigma_3 \left[ \frac{\omega}{2} - \frac{\sqrt{\pi}\tilde{V}}{2}(\cos p_x + \cos p_y) \right] \right] \quad (38)$$

$$\tilde{V} = V_{10}e^{-\frac{1}{2}\pi}\sqrt{\pi} \quad (39)$$

The ground state of  $H^I(\mathbf{p})$  will be referred to as the Modified LLL, or MLLL. It is our Chern band. The function  $g(\mathbf{p})$  affects the energy dispersion of the MLLL, but not the Chern density  $\mathcal{B}(\mathbf{p})$ .

Though  $H^I(\mathbf{p})$  has the form of the Lattice Dirac Model (Eq. 23), it is in the topologically trivial region. This is due to our requirement  $\omega > 2\sqrt{\pi}\tilde{V}$  which ensures that the two bands do not touch at  $p_x = p_y = 0$ , which in turn ensures that the Chern number remains  $\mathcal{C} = -1$ . Due to the topological triviality of  $H^I(\mathbf{p})$  the pseudo-spin  $\mathbf{n}(\mathbf{p}) = \langle u(\mathbf{p}) | \boldsymbol{\sigma} | u(\mathbf{p}) \rangle$  never enters the southern hemisphere. Nonetheless the overall  $\mathcal{C} = -1$  because *nontrivial topology is contained in the  $\mathbf{p}$ -dependent basis functions*. Whereas in the traditional LDM, the tight binding wavefunctions are  $\mathbf{p}$ -independent spinors,  $[1, 0]^T$  and  $[0, 1]^T$ , here they are the states  $|\mathbf{p}, n = 0, 1\rangle$  with topologically nontrivial  $\mathbf{p}$  dependence. The total  $\mathcal{B}$  in this problem has a constant piece  $-\frac{1}{2\pi}$  coming from the basis functions and responsible for  $\mathcal{C} = -1$ , and two more  $\mathbf{p}$ -dependent terms with zero integrals: one due to the  $\mathbf{p}$ -dependence of the ground state spinor, and a cross term that arises because  $\langle n | \nabla_p | n' \rangle \neq 0$  for  $n \neq n'$ . The total  $\mathcal{B}(\mathbf{p})$  is shown in Figure 2 along with the Chern density for the LDM at  $M = 1$ . Notice the strong similarity even in this minimal model with just two LLs and one harmonic in  $V$ .

Now that we have a nontrivial Chern band with a nonconstant  $\mathcal{B}(\mathbf{p})$  let us proceed to the CF-substitution, which will in turn lead us to the gapped state in the HF approximation at  $\nu = \frac{1}{3}$  when interactions are turned on.

First we need to find  $\rho_{\text{MLLL}}$ , the projection of the electron density operator to the Chern band, the MLLL. When  $V_{10} = 0$ , clearly  $\rho_{\text{MLLL}}(\mathbf{q}) = \rho_{\text{LLL}}(\mathbf{q})$ . To find out what it is when  $V_{10}$  is turned on we proceed as follows:

- Find the  $2 \times 2$  matrix that describes the electron density  $\rho_e(\mathbf{q}) = e^{i\mathbf{q}\cdot\mathbf{r}_e}$  in the space of the LLs,  $n = 0, 1$ .
- Find the eigenstates of  $H^I(\mathbf{p})$ .
- Project  $\rho_e(\mathbf{q}) = e^{i\mathbf{q}\cdot\mathbf{r}_e}$  to the ground state at each  $\mathbf{p}$ , the MLLL.

The matrix elements of  $\rho_e(\mathbf{q}) = e^{i\mathbf{q}\cdot\mathbf{r}_e}$  between the magnetic Bloch states defined in Eq. 28 vanish unless the initial momentum  $\mathbf{p}$  and final momentum  $\mathbf{p}'$ , both restricted to the BZ, obey

$$\mathbf{p}' = [\mathbf{p} + \mathbf{q}] = (\mathbf{p} + \mathbf{q}) \mod \mathbf{G} \quad (40)$$

Thus we must subtract from  $\mathbf{p} + \mathbf{q}$  that  $\mathbf{G}$  which restricts  $\mathbf{p}'$  to the BZ.

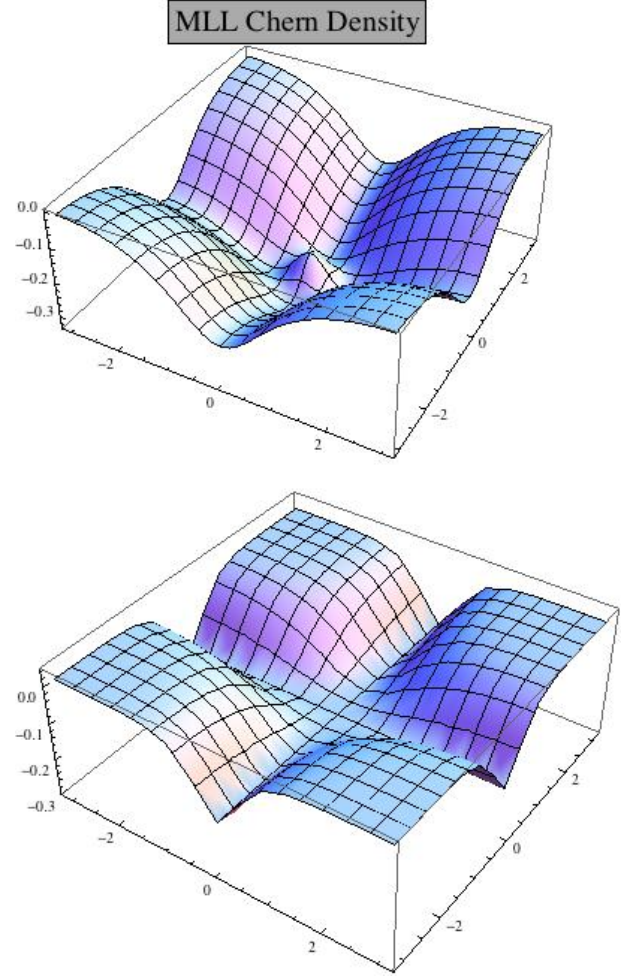


FIG. 2: Top:  $\mathcal{B}(\mathbf{p})$  in the MLLL with just two LLs and one harmonic  $V_{01} \neq 0$ . Bottom: Berry flux density in the Lattice Dirac Model at  $M = 1$ .

$$2\pi N_x \mathbf{e}_x + 2\pi N_y \mathbf{e}_y = \mathbf{p} + \mathbf{q} - [\mathbf{p} + \mathbf{q}] \quad (41)$$

The non-zero matrix elements are found to be

$$\langle [\mathbf{p} + \mathbf{q}] n_2 | e^{i\mathbf{q}\cdot\mathbf{r}_e} | \mathbf{p} n_1 \rangle = \\ \rho_{n_2 n_1} \exp \left[ \frac{i}{2\pi} \left( \frac{1}{2} q_x q_y + q_x p_y - (p_x + q_x) 2\pi N_y \right) \right] \\ \equiv \rho_{n_2 n_1}(\mathbf{q}) e^{i\Phi(\mathbf{q}, \mathbf{p})} \quad (42)$$

where  $\rho_{n_2 n_1}(\mathbf{q})$  has been defined in Eq. 37. The asymmetry between  $p_x$  and  $p_y$  in Eq. 42 reflects our choice of the Landau gauge in defining the basis states in Eq. 28.

In view of its importance to what follows we display  $e^{i\Phi(\mathbf{q}, \mathbf{p})}$  prominently below:

$$e^{i\Phi(\mathbf{q}, \mathbf{p})} = \exp \left[ \frac{i}{2\pi} \left( \frac{1}{2} q_x q_y + q_x p_y - (p_x + q_x) 2\pi N_y \right) \right] \quad (43)$$

The corresponding second-quantized operator is

$$\rho_e(\mathbf{q}) = \sum_{\mathbf{p}} \sum_{n_1, n_2=0,1} a_{n_2}^\dagger([\mathbf{p} + \mathbf{q}]) \rho_{n_2 n_1}(\mathbf{q}) a_{n_1}(\mathbf{p}) e^{i\Phi(\mathbf{q}, \mathbf{p})} \quad (44)$$

where  $a_n$  and  $a_n^\dagger$  are the operators associated with the basis states  $|\mathbf{p}n\rangle$ .

Let  $U$  be the matrix that diagonalizes  $H^I(\mathbf{p})$  in Eq. 38 and relates  $a_n$  to the  $d_n$  associated with the energy eigenstates as follows

$$\begin{pmatrix} a_0(\mathbf{p}) \\ a_1(\mathbf{p}) \end{pmatrix} = \begin{pmatrix} U_{00} & U_{01} \\ U_{10} & U_{11} \end{pmatrix} \begin{pmatrix} d_0(\mathbf{p}) \\ d_1(\mathbf{p}) \end{pmatrix} \quad (45)$$

Since  $H^I(\mathbf{p})$  is topologically trivial,  $U$ , like the eigenspinors, is globally defined in the BZ and periodic in  $\mathbf{p}$ . Switching to the new basis and projecting to the ground state we obtain

$$\begin{aligned} \rho_{\text{MLLL}}(\mathbf{q}) &= \sum_{\mathbf{p}} d_0^\dagger(\mathbf{p}') d_0(\mathbf{p}) e^{i\Phi(\mathbf{q}, \mathbf{p})} f(\mathbf{q}, \mathbf{p}) \\ f(\mathbf{q}, \mathbf{p}) &= U_{0n'}^\dagger(\mathbf{p}') \rho_{n'n}(\mathbf{q}) U_{n0}(\mathbf{p}) \end{aligned} \quad (46)$$

Hereafter the subscript on  $d_0$ , indicating that it corresponds to the ground state or MLLL, will be dropped.

Thus we have a Chern band, a non-constant  $\mathcal{B}$  and a closed expression for the projected density. The final step before we carry out the CF substitution is to write this density in terms of  $\rho_{\text{GMP}}$ . Before doing this explicitly, we provide an intuitive argument that this can be done. When  $V_{10} = 0$ , we know  $\rho_{\text{MLLL}} = e^{-q^2 l^2/4} \rho_{\text{GMP}}$ . As we turn on  $V_{10}$ , the perturbing terms are of the form  $e^{i\mathbf{G}_0 \cdot \mathbf{r}_e} = e^{i\mathbf{G}_0 \cdot \boldsymbol{\eta}_e} e^{i\mathbf{G}_0 \cdot \mathbf{R}_e}$  where  $\mathbf{G}_0 = 2\pi(\mathbf{e}_x n_x + \mathbf{e}_y n_y)$  with only one of  $n_x$  or  $n_y = \pm 1$ . Given the GMP algebra, the repeated action of this perturbation can only be to turn  $\rho_{\text{GMP}}(\mathbf{q})$  into a sum over  $\rho_{\text{GMP}}(\mathbf{q} + \mathbf{G})$ , where  $\mathbf{G}$  is now any reciprocal lattice vector. So we do expect that in the end, even for an arbitrary periodic potential

$$\rho_{\text{MLLL}}(\mathbf{q}) = \sum_{\mathbf{G}} c(\mathbf{G}, \mathbf{q}) \rho_{\text{GMP}}(\mathbf{q} + \mathbf{G}) \quad (47)$$

Since the bands never touch, perturbation theory will always converge. However the final result is non-perturbative and follows simply from the dependence of  $H^I(\mathbf{p})$  on  $e^{i\mathbf{G}_0 \cdot \mathbf{R}_e}$ .

We will now show Eq. 47 explicitly and compute  $c(\mathbf{G}, \mathbf{q})$ .

First let us construct an auxiliary operator which obeys the GMP algebra.

$$\rho_{\text{GMP}}(\mathbf{q}) = \sum_{\mathbf{p}} d^\dagger(\mathbf{p}') d(\mathbf{p}) e^{i\Phi(\mathbf{q}, \mathbf{p})} \quad (48)$$

Given any BZ in which the operators  $d, d^\dagger$  appearing in Eq. 48 are canonical, it is easily verified that this operator satisfies the magnetic translation algebra Eq. 1. We likewise construct operators with momenta

$$\mathbf{q} + \mathbf{G} = \mathbf{q} + 2\pi n_x \mathbf{e}_x + 2\pi n_y \mathbf{e}_y : \quad (49)$$

defined by

$$\begin{aligned} \rho_{\text{GMP}}(\mathbf{q} + \mathbf{G}) &= \sum_{\mathbf{p}} d^\dagger(\mathbf{p}') d(\mathbf{p}) e^{i\Phi(\mathbf{q} + \mathbf{G}, \mathbf{p})} \\ &= \sum_{\mathbf{p}} d^\dagger(\mathbf{p}') d(\mathbf{p}) e^{i\Phi(\mathbf{q}, \mathbf{p})} e^{\frac{i}{2}(q_y n_x - q_x n_y + 2\pi n_x n_y)} e^{-ip_x n_y + ip_y n_x} \end{aligned} \quad (50)$$

Note that whether we transfer momentum  $\mathbf{q}$  or  $\mathbf{q} + \mathbf{G}$  to  $\mathbf{p}$  the resultant  $\mathbf{p}'$  is the same. *We emphasize that these operators can be constructed for any problem in a square lattice BZ, with no reference to any LLs.* This fact will be crucial in the next section.

We now give the details of the counting argument that assures us that  $\rho_{\text{MLLL}}(\mathbf{q})$  may be expanded in terms of  $\rho_{\text{GMP}}(\mathbf{q} + \mathbf{G})$ . Consider a system of size  $L \times L$  wrapped into a torus. The question to ask is: For a given  $\mathbf{q}$  in the BZ, for how many different values of  $\mathbf{G}$  are the  $\rho_{\text{GMP}}(\mathbf{q} + \mathbf{G})$  linearly independent? Since  $a = 1$ , the number of sites is  $N^2 = \frac{L^2}{a^2} = L^2$ , which also equals the number of points in the BZ, the number of distinct values for  $\mathbf{p}$  and the number of distinct values of  $\mathbf{q}$  in the lattice model. The smallest value for any component of  $\mathbf{q}$  or  $\mathbf{p}$  is  $q_{\min} = p_{\min} = \frac{2\pi}{L}$ . To verify that the largest distinct value for any component of  $\mathbf{G}$  is  $G_{\max} = 2\pi N$ , consider the second and third exponentials in Eq. 50 which alone depend on  $\mathbf{G}$ . Focus on a factor like  $e^{-\frac{i}{2}q_x n_y}$  when  $q_x = q_{\min}$  and  $n_y = N$

$$e^{-\frac{i}{2}q_x n_y} \Big|_{q_x = \frac{2\pi}{L}, n_y = N} = e^{-i\pi \frac{N}{L}} = -1. \quad (51)$$

The same goes for all the terms in the second exponential, while the third exponential always equals unity, which means

$$\rho_{\text{GMP}}(\mathbf{q} + \mathbf{G}_{\max}) \propto \rho_{\text{GMP}}(\mathbf{q}) \quad (52)$$

Thus we get linearly independent densities only for components up to  $G_{\max} = 2\pi N$ . There are only  $N^2$  independent values of  $\mathbf{G}$ , just as for  $\mathbf{p}$  or  $\mathbf{q}$ . But this means there are  $N^4$  linearly independent operators of the form  $\rho_{\text{GMP}}(\mathbf{q} + \mathbf{G})$ , exactly the right number to form a basis, like the canonical basis  $d_{\mathbf{p}_2}^\dagger d_{\mathbf{p}_1}$ . So what we find is that not only  $\rho_{\text{FCB}}$ , but any bilinear operator  $O$  (such as the lattice current operator) of the form  $\sum_{\mathbf{p}} d^\dagger(\mathbf{p}') d(\mathbf{p}) O(\mathbf{q}, \mathbf{p})$  can be expanded in terms of  $\rho_{\text{GMP}}(\mathbf{q} + \mathbf{G})$ .

Having hammered home our central point, we now turn to the determination of the coefficients of the expansion. To this end we combine Eqs. 46, 47 and 50 and write

### A. The CF substitution

$$\begin{aligned} \rho_{\text{MLLL}}(\mathbf{q}) &= \sum_{\mathbf{p}} d^\dagger(\mathbf{p}') d(\mathbf{p}) e^{i\Phi(\mathbf{q}, \mathbf{p})} f(\mathbf{q}, \mathbf{p}) \end{aligned} \quad (53)$$

$$\begin{aligned} &= \sum_{\mathbf{p}} \sum_{n_x, n_y} c(n_x, n_y, \mathbf{q}) d^\dagger(\mathbf{p}') d(\mathbf{p}) e^{i\Phi(\mathbf{q}, \mathbf{p})} \\ &\times e^{\frac{i}{2}(-q_x n_y + q_y n_x + 2\pi n_x n_y)} e^{-ip_x n_y + ip_y n_x} \end{aligned} \quad (54)$$

This equation can of course be satisfied since

$$\begin{aligned} f(\mathbf{q}, \mathbf{p}) &= \sum_{n_x, n_y} c(n_x, n_y, \mathbf{q}) \\ &\times e^{\frac{i}{2}(-q_x n_y + q_y n_x + 2\pi n_x n_y)} e^{-ip_x n_y + ip_y n_x} \end{aligned} \quad (55)$$

is, at each  $\mathbf{q}$ , just the Fourier expansion of the function  $f$  periodic in  $\mathbf{p}$  in terms of oscillating exponentials of the first period.

The commutators of the projected electron density  $\rho_{\text{MLLL}}(\mathbf{q})$  can be worked out, if desired. They will be neither pretty nor universal<sup>19</sup>, unlike the magnetic translation algebra<sup>20</sup>, depending instead on the details of the lattice via  $f(\mathbf{q}, \mathbf{p})$ .

Having expressed  $\rho_{\text{MLLL}}(\mathbf{q})$  in terms of  $\rho_{\text{GMP}}(\mathbf{q} + \mathbf{G})$  we need to do the same for a term in  $\bar{H}$  that is absent in the usual LLL: the non-constant kinetic energy  $-\varepsilon(\mathbf{p})$  of the MLLL. Because  $\varepsilon(\mathbf{p})$  is periodic mod  $\mathbf{G}$ , this is a special case ( $\mathbf{q} = 0$ ) of the Fourier transform we carried out for  $\rho_{\text{MLLL}}(\mathbf{q})$ . We write

$$\begin{aligned} &-\sum_{\mathbf{p}} d^\dagger(\mathbf{p}) d(\mathbf{p}) \varepsilon(\mathbf{p}) \\ &= \sum_{\mathbf{G}} h(\mathbf{G}) \rho_{\text{GMP}}(\mathbf{G}) \\ &= \sum_{n_x, n_y} d^\dagger(\mathbf{p}) d(\mathbf{p}) h(n_x, n_y) e^{-ip_x n_y + ip_y n_x + i\pi n_x n_y} \end{aligned} \quad (56)$$

which amounts to Fourier expanding the energy dispersion  $-\varepsilon(\mathbf{p})$ . We now have the full electronic hamiltonian for the FCB in terms of  $\rho_{\text{GMP}}$ .

Note that the phase factor

$$e^{i\Phi(\mathbf{q}, \mathbf{p})} = \exp \left[ \frac{i}{2\pi} \left( \frac{1}{2} q_x q_y + q_x p_y - (p_x + q_x) 2\pi N_y \right) \right] \quad (58)$$

jumps in  $\mathbf{p}$  space for a fixed  $\mathbf{q}$ . For example if  $\mathbf{q} = 3\mathbf{e}_y$  and the BZ is in the interval  $[0 - 2\pi]$  in both directions, then for any  $\mathbf{p}$  with  $p_y > 2\pi - 3$ , adding  $\mathbf{q}$  will take it to the next BZ and  $N_y$  will have to jump from 0 to 1 to bring  $\mathbf{p}'$  within the BZ. *Luckily, this discontinuous  $\Phi$  and its jump are shared by both  $\rho_{\text{MLLL}}(\mathbf{q})$  and  $\rho_{\text{GMP}}(\mathbf{q} + \mathbf{G})$  as we find in Eqs. 53 and 54. This ensures rapid convergence of the Fourier expansion of the jump-free part  $f(\mathbf{q}, \mathbf{p})$  in Eq. 55.*

Now we must switch to CFs. We only sketch the broad ideas. We consider the case of  $\nu = \frac{1}{3}$  when the CF has a charge  $e^* = \frac{1}{3}e$  and  $l^{*2} = 3l^2 = \frac{3}{2\pi}$ . The spatial unit cell is 3 units long in the x-direction so as to enclose unit flux *as seen by the CF* so that  $BZ_{\text{CF}}$  goes from  $-\frac{\pi}{3} \leq p_x \leq \frac{\pi}{3}$  and is unchanged in the y-direction. However when we construct the projected electron density operators we will need to consider  $\mathbf{q}$  that runs over the BZ of the electron not the CF.

Consider  $\rho_{\text{GMP}}(\mathbf{q})$  which was  $e^{i\mathbf{q} \cdot \mathbf{R}_e}$  in first quantization and

$$\begin{aligned} \rho_{\text{GMP}}(\mathbf{q}) &= \sum_{\mathbf{p} \in BZ_e} d^\dagger(\mathbf{p}') d(\mathbf{p}) \\ &\times \exp \left[ \frac{i}{2\pi} \left( \frac{1}{2} q_x q_y + q_x p_y - (p_x + q_x) 2\pi N_y \right) \right] \end{aligned} \quad (59)$$

in second quantization. To go to the CF representation means to write

$$e^{i\mathbf{q} \cdot \mathbf{R}_e} = e^{i\mathbf{q} \cdot (\mathbf{R} + \boldsymbol{\eta}c)} \quad (60)$$

in first quantization and the following representation in terms of CF operators  $C$  and  $C^\dagger$  in second quantization

$$\begin{aligned} \rho_{\text{GMP}}(\mathbf{q}) &= \sum_{\mathbf{p} \in BZ_{\text{CF}}} C_{n'}^\dagger(\mathbf{p}') C_n(\mathbf{p}) \rho_{n'n}(\mathbf{q} \rightarrow c\mathbf{q}, l \rightarrow l^*) \\ &\times \exp \left[ \frac{3i}{2\pi} \left( \frac{1}{2} q_x q_y + q_x p_y - (p_x + q_x) 2\pi N_y \right) \right] \end{aligned} \quad (61)$$

where the 3 is due to  $l^{*2} = 3l^2 = \frac{3}{2\pi}$ , and the argument of  $\rho_{n'n}$  is  $\mathbf{q}c$  because the  $c$  in  $\boldsymbol{\eta}c$  may be lumped with  $\mathbf{q}$  (see Eq. 21). Note that all CF-LLs ( $n = 0, 1, \dots$ ) appear in the density, a result of the enlarged Hilbert space in which we are representing the problem.

With the Hamiltonian expressed in terms of CF operators, we move to the HF calculation. We set  $\omega = 10$  (the gap between the two electronic LLs) and choose the periodic potential to be  $V_{\text{PP}} = V_{10} e^{-\frac{1}{2}\pi} = 1$ . We keep 3 CF-LLs which get mixed by the periodic potential and interaction. We end up with three bands which are fairly well separated. Unlike in the continuum where the CF-LLs were uniformly filled, the occupation number here varies with  $\mathbf{p}$  (due to the periodic potential) and had to be found self-consistently. Figure 3 shows the results of our calculation for the coulomb interaction of strength  $\frac{2\pi V_{ee}}{q}$ . We see a clear gap separating the lowest band which is fully occupied from the others, even at very small values of  $V_{ee}$ .

This is puzzling since one expects the CF-picture to break down for  $V_{ee} \ll V_{\text{PP}}$ . Upon further investigation we found two signals that point to the breakdown of the CF picture, one internal and one external.



### Hartree Fock Bands, $\nu=1/3$

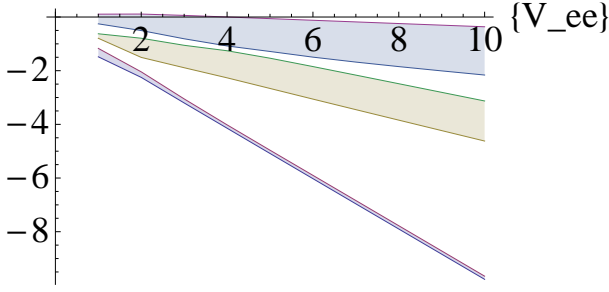


FIG. 3: The results of our Hartree Fock calculation at  $\nu = \frac{1}{3}$  and  $\omega = 10$ , for the Coulomb interaction  $\frac{2\pi V_{ee}}{q}$ . The three bands resulting from three CF-LLs which get mixed and modulated by the periodic potential  $V_{PPP} = 1$ .

The internal one involves the occupation numbers of the CF-LLs in the ground state at each  $\mathbf{p}$ . Figure 4 shows that at  $V_{ee} = 10$ ,  $n_{CF} = 0, 1$  are robustly occupied while  $n_{CF} = 2$  has negligible occupancy. Thus our truncation with three CF-LLs is safe, since the  $n = 2$  level is not called into play. By contrast at  $V_{ee} = 0.5$  we see in Figure 5 that occupation of  $n_{CF} = 2$  can be substantial. The levitation of the fermions to the upper CF-LLs is a clear indication that CF theory is failing as a good low-energy theory.

Before moving to the external signature, let us observe a three-fold symmetry in the occupations as a function of  $p_y$ , which is also reflected in the energy bands. This is a consequence of the  $x$ -translation symmetry of the noninteracting Hamiltonian<sup>37</sup>. Recall that  $T_x$  commutes with the Hamiltonian, but not with  $T_y$ . It can be easily shown that

$$T_x |p_x, p_y, n\rangle = e^{i\phi(\mathbf{p})} |p_x, p_y - \frac{2\pi}{3}, n\rangle \quad (62)$$

This symmetry is also possessed by the HF Hamiltonian

$$T_x^\dagger H_{HF}(p_x, p_y) T_x = H_{HF}(p_x, p_y - \frac{2\pi}{3}) \quad (63)$$

and thus by the energy bands and the occupations.

Now we turn to the external test that signals the breakdown of the CF state and is sharper than the one based on occupation numbers. It involves the comparison of the variational energy per particle in the FCI state and the electronic Fermi liquid state. It is clear that the energy of the electronic Fermi liquid state (which lies in the physical Hilbert space) provides a variational upper bound for the exact ground state energy. It is not so clear that the energy of the CF state, which is defined in a bigger space containing the physical coordinate  $\mathbf{R}_e$  and the unphysical vortex coordinates  $\mathbf{R}_v$ , is variational. One might worry that these extra unphysical degrees of freedom may allow a further lowering of energy not permitted in the physical sector. This is, however, not true. Since the hamiltonian in the enlarged space depends only

### Occupations $n=0,1,2$ , $V_{ee} = 10.0$ , $V_{PP}=1$

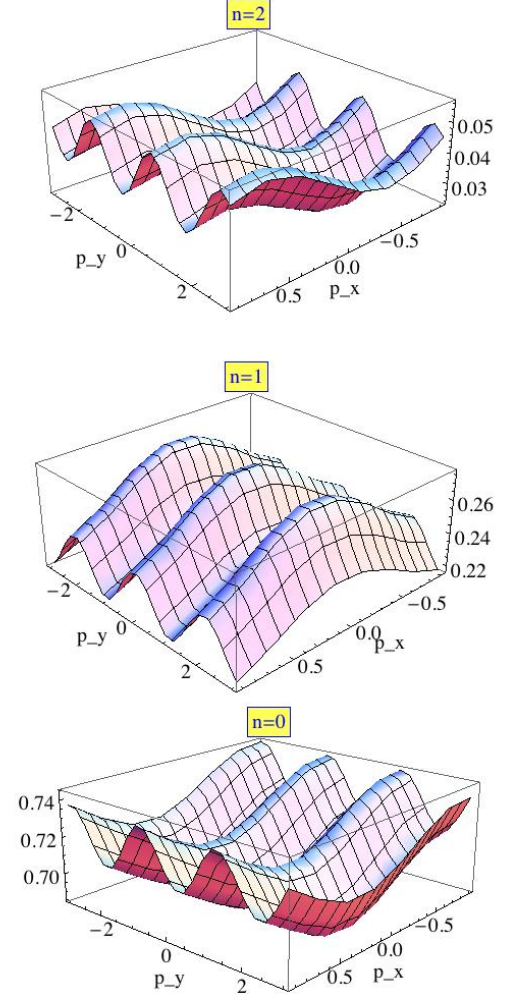


FIG. 4: The occupation numbers in CF-LLs 0,1, and 2 at  $V_{ee} = 10, V_{PP} = 1, \omega = 10$ . Notice that the  $n = 0, 1$  levels (bottom two) saturate the occupancy while the  $n = 2$  (top) level is practically empty, validating the truncation at three CF-LLs and establishing CF theory as a good low-energy description. The plots repeat three times in the  $p_y$  direction because  $T_x$  and  $T_x^2$  commute with  $H$ , but do not commute with  $T_y$  and add  $\frac{2\pi}{3}$  and  $\frac{4\pi}{3}$  to  $p_y$ , respectively.

on the electronic guiding center coordinate  $\mathbf{R}_e$  via  $\rho_{GMP}$  and is independent of the vortex coordinate  $\mathbf{R}_v$ , the exact eigenfunctions must be tensor products of the exact eigenfunctions in the physical sector and arbitrary wavefunctions in the unphysical sector. However, the energy is independent of the choice made in the unphysical sector. Thus the exact ground state energy in the enlarged space is equal to that in the physical sector and consequently *any function in the enlarged space can furnish a variational upper bound to the exact ground state energy*. We compute the energy of the HF ground state with one filled CF-LL. This, of course, is not an exact



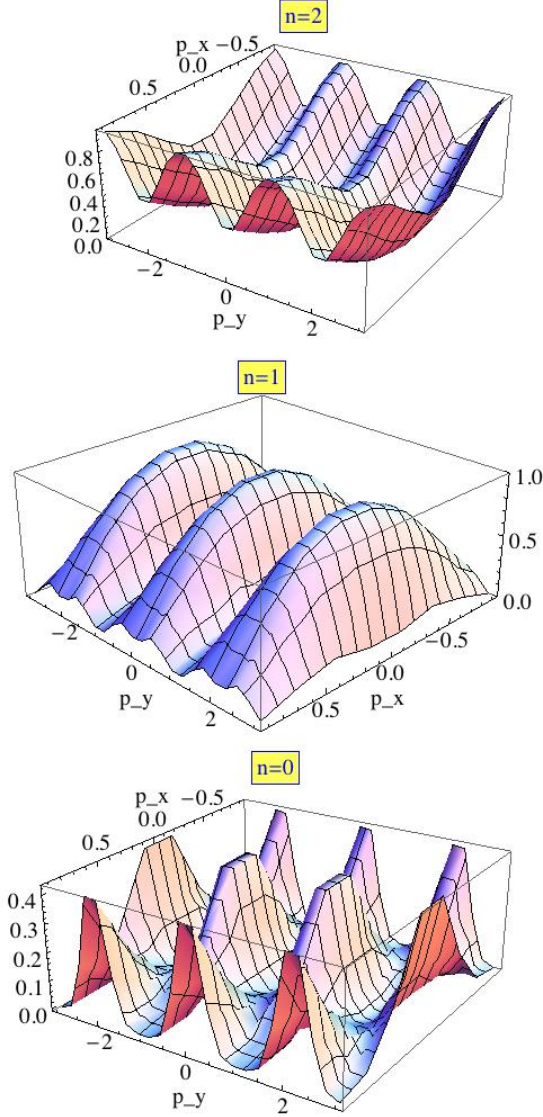
Occupations  $n=0,1,2$ ,  $V_{ee} = 0.5$ ,  $V_{PP}=1$ 

FIG. 5: The occupation numbers in CF-LLs 0,1, and 2 at  $V_{ee} = 0.5$ ,  $V_{PP} = 1$ ,  $\omega = 10$ . Notice that the particles are levitating towards the  $n = 2$  level (top) and moving away from  $n = 0$ , which calls the truncation at three CF-LLs into question. The plots repeat three times in the  $p_y$  direction because  $T_x$  and  $T_x^2$  which do not commute with  $T_y$  add  $\frac{2\pi}{3}$  and  $\frac{4\pi}{3}$  to  $p_y$ , respectively, commute with  $H$ .

eigenfunction. In fact, it is not even in the form of a tensor product between the physical and unphysical sectors, being instead a linear combination of tensor product states. However, by the above argument, it nevertheless provides a variational upper bound on the exact ground state energy. Fig. 6 shows the the HF energy per particle of the Fermi liquid (smaller dots) versus to  $\frac{1}{3}$  FCI state (larger dots). We see that the Fermi liquid yields to the FCI state at  $V_{ee} \simeq 2.5$ . We caution the reader that this

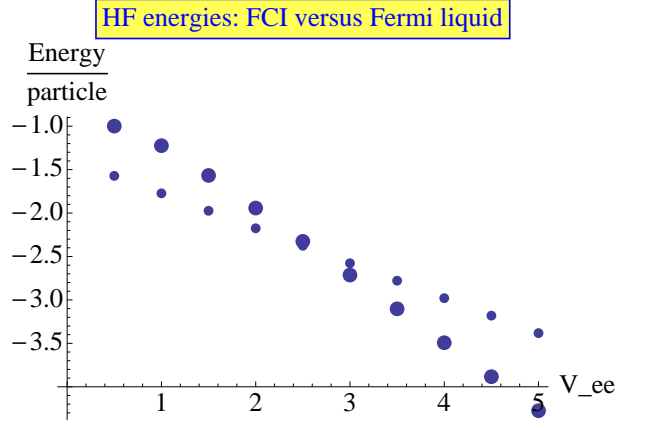


FIG. 6: Comparison of the HF energy per particle of the electronic Fermi liquid (smaller dots) versus the  $\frac{1}{3}$  FCI state (larger dots). We see that the Fermi liquid, which wins at small interaction strength  $V_{ee}$  yields to the FCI state around  $V_{ee} = 2.5$ .

does not mean that the FCI state unequivocally wins. It is possible that there are correlated *electronic* states with an even lower energy that our CF-state.

To summarize, we produced a non-trivial Chern band by transferring the topology to the basis functions in  $\mathbf{p}$  space. These functions arose from two electronic LLs mixed by a periodic potential. The projected charge density at momentum  $\mathbf{q}$  was then written as a computable sum over  $\mathbf{G}$  of GMP densities at  $\mathbf{q} + \mathbf{G}$ . The GMP densities were treated in the Hamiltonian method by the replacement  $\mathbf{R}_e = \mathbf{R} + \boldsymbol{\eta}c$ . Finally a HF calculation was carried out using a gapped CF ground state. We see that although a FCI state always exists, even for very weak interactions  $V_{ee}$ , the occupations of the higher CF-LLs becomes smaller with increasing  $V_{ee}$ , providing an internal signal of its stability. A sharper limit for the goodness of the FCI state is provided by the comparison to the variational energy of the electronic Fermi liquid state, which wins for  $V_{ee} < 2.5$ , but gets bested by the FCI state for larger  $V_{ee}$ .

## B. Variants and limitations of Type I models

A natural extension of the above example is to impose more complicated periodic potentials to get more complicated  $\mathcal{B}(\mathbf{p})$ s. Earlier in our exploration<sup>38</sup> we pursued this line of thought so as to reproduce the  $\mathcal{B}(\mathbf{p})$  of some specific lattice model, say the LDM. (We see in Fig. 2 that the  $\mathcal{B}(\mathbf{p})$  of the MLLL with just one harmonic is already not too different from that of the LDM.) Our motivation was as follows. *Let us take the view that the FCB problem is defined by (i)  $\mathcal{B}(\mathbf{p})$  and (ii) the interaction written in terms of the projected density  $\rho_{FCB}(\mathbf{q})$ .* The logic behind (i) is that the projected electron coordinate

$$(R_{\mu}^{FCB})_{\mathbf{p}\mathbf{p}'} = (i\frac{\partial}{\partial p_{\mu}} + \mathcal{A}_{\mu}(\mathbf{p}))\delta^2(\mathbf{p} - \mathbf{p}') \quad (64)$$

has commutators defined by  $\mathcal{B}$ :

$$[R_x^{FCB}, R_y^{FCB}]_{\mathbf{p}\mathbf{p}'} = i\mathcal{B}(\mathbf{p})\delta^2(\mathbf{p} - \mathbf{p}') \quad (65)$$

It follows that if we can construct a surrogate band with the same  $\mathcal{B}(\mathbf{p})$  as in a given FCB, *then any function of the projected electron coordinates will be algebraically the same in the two problems.*

Let us review where this line of thought leads in the continuum FQH problem. There we represent the electron's projected coordinate  $\mathbf{R}_e$  in terms of CF variables  $\mathbf{R}$  and  $\boldsymbol{\eta}$ . Getting the algebra of  $\mathbf{R}_e$  correctly also means getting the algebra of  $\rho_{\text{LLL}}$ , the projected density right, up to a known prefactor. Thus, if  $\langle \dots \rangle$  denotes averages in the target band, which here is the LLL,

$$\mathbf{r}_e = \mathbf{R}_e + \boldsymbol{\eta}_e \quad \text{which implies} \quad (66)$$

$$\langle \mathbf{r}_e \rangle = \mathbf{R}_e \quad \text{while} \quad (67)$$

$$\langle e^{i\mathbf{q} \cdot \mathbf{r}_e} \rangle = \langle e^{i\mathbf{q} \cdot (\mathbf{R}_e + \boldsymbol{\eta}_e)} \rangle \quad (68)$$

$$= \langle e^{i\mathbf{q} \cdot \boldsymbol{\eta}_e} \rangle e^{i\mathbf{q} \cdot \mathbf{R}_e} \quad (69)$$

$$= e^{-q^2 l^2 / 4} e^{i\mathbf{q} \cdot \langle \mathbf{r}_e \rangle} \quad (70)$$

In other words, the projection of the exponential of  $\mathbf{r}_e$  is, up to a known prefactor  $e^{-q^2 l^2 / 4}$ , the same as the exponential of the projection because  $\boldsymbol{\eta}_e$  and  $\mathbf{R}_e$  commute. This is why if the projected coordinate is faithfully represented, so is the projected density. We go over these well known facts to highlight the unusual simplicity of projecting to the LLL.

Unfortunately, in the generic FCB problem this is no longer true. Let us define two different projected densities in the FCB. One is the usual one:

$$\rho_{\text{FCB}}(\mathbf{q}) = \langle \text{FCB} | e^{i\mathbf{q} \cdot \mathbf{r}_e} | \text{FCB} \rangle \quad (71)$$

This is the projected density which enters the interacting Hamiltonian in the FCB.

The other is the analogue of the guiding center density:

$$\bar{\rho}_{\text{FCB}}(\mathbf{q}) = e^{i\mathbf{q} \cdot \mathbf{R}_e^{\text{FCB}}} \quad (72)$$

In the FCB problem

$$\rho_{\text{FCB}}(\mathbf{q}) \neq C(q)\bar{\rho}_{\text{FCB}}(\mathbf{q}) \quad (73)$$

because the “guiding center” coordinates  $\mathbf{R}^{\text{FCB}}$  do not commute with the analogue of the cyclotron coordinates. *Thus,  $\mathcal{B}(\mathbf{p})$  is not enough to specify the interacting Hamiltonian in the FCB completely. One needs the expression for  $\rho_{\text{FCB}}(\mathbf{q})$  as well.*

However, to lowest order in  $\mathbf{q}$  and  $\mathbf{q}'$  we have, in first quantization and in  $\mathbf{p}$ -space,

$$[\rho_{\text{FCB}}(\mathbf{q}), \rho_{\text{FCB}}(\mathbf{q}')] = -i[\mathbf{q} \times \mathbf{q}'] \mathcal{B}(\mathbf{p}) + \text{higher order terms} \quad (74)$$

as pointed out by Parameswaran *et al*<sup>19</sup>.

So if the Chern flux density  $\mathcal{B}(\mathbf{p})$  of the surrogate band matches that of the lattice FCB,  $\rho_{\text{FCB}}(\mathbf{q})$  and  $\bar{\rho}_{\text{FCB}}(\mathbf{q})$  will bear a close resemblance to each other but not be equal in all respects. Since these are both models anyway, one may argue that it is sufficient to get a surrogate that approximates the original lattice model and is yet amenable to analytic treatment. However we will not pursue this approach further since there is a more direct way to obtain  $\rho_{\text{FCB}}(\mathbf{q})$  in terms of  $\rho_{\text{GMP}}(\mathbf{q})$  for an arbitrary lattice model, which we now describe.

### III. TYPE II MODELS

In the previous section we showed how to carry out the CF substitution in LL-based models with nonconstant  $\mathcal{B}(\mathbf{p})$ . In this section we present a more general approach for incorporating CFs in the solution of any *given* lattice model with a Chern band, without any reference to LLs. We illustrate this approach by considering the LDM with some interaction  $V_{ee}$ .

Here are the concrete set of steps we follow:

- Construct  $\rho_{\text{FCB}}(\mathbf{q})$ , the projected density operator in terms of the eigenfunctions of noninteracting LDM hamiltonian  $H(\mathbf{p})$  and the operators  $d$  and  $d^\dagger$  associated with the Chern band at each  $\mathbf{p}$ .
- Construct operators obeying the algebra of  $\rho_{\text{GMP}}(\mathbf{q} + \mathbf{G})$  using  $d$  and  $d^\dagger$  as per Eq. 50. As noted immediately after that equation, this can always be done. To get the best possible results this must be done in  $A_y = 0$  gauge.
- Expand as before, using the complete set of  $N^4$  operators  $\rho_{\text{GMP}}(\mathbf{q} + \mathbf{G})$ :

$$\rho_{\text{FCB}}(\mathbf{q}) = \sum_{\mathbf{G}} c(\mathbf{G}, \mathbf{q}) \rho_{\text{GMP}}(\mathbf{q} + \mathbf{G}). \quad (75)$$

This will be just a Fourier expansion in  $e^{ip_x n_y - ip_y n_x}$ .

- Carry out the CF substitution in  $\rho_{\text{GMP}}$  and go on to the HF approximation.

We illustrate the above steps with the LDM at  $M = 1$ :

$$H(\mathbf{p}) = \sigma_1 \sin p_x + \sigma_2 \sin p_y + \sigma_3 (1 - \cos p_x - \cos p_y) \quad (76)$$

with ground-state energy

$$-\varepsilon(\mathbf{p}) = -\sqrt{1 + 2(1 - \cos p_x)(1 - \cos p_y)}. \quad (77)$$

The generic formula for the projected charge density is

$$\rho_{\text{FCB}}(\mathbf{q}) = \sum_{\mathbf{p}} d^\dagger([\mathbf{p} + \mathbf{q}]) d(\mathbf{p}) \langle [\mathbf{p} + \mathbf{q}] | \mathbf{p} \rangle \quad (78)$$

where  $d^\dagger, d$  create and destroy the ground state and  $|\mathbf{p}\rangle$  is the corresponding Bloch spinor. However  $|\mathbf{p}\rangle$  is not

globally defined<sup>39</sup> over the BZ because  $\mathcal{C} = -1$ . Here are two choices that work in two different patches:

$$|\mathbf{p}\rangle_1^0 = \begin{pmatrix} \sin \frac{\theta(\mathbf{p})}{2} \\ -\cos \frac{\theta(\mathbf{p})}{2} e^{i\phi(\mathbf{p})} \end{pmatrix} \quad (79)$$

$$|\mathbf{p}\rangle_2^0 = \begin{pmatrix} \sin \frac{\theta(\mathbf{p})}{2} e^{-i\phi(\mathbf{p})} \\ -\cos \frac{\theta(\mathbf{p})}{2} \end{pmatrix} \quad (80)$$

where

$$\cos \theta(\mathbf{p}) = \frac{1 - \cos p_x - \cos p_y}{\varepsilon(\mathbf{p})} \quad (81)$$

$$e^{i\phi(\mathbf{p})} = \frac{\sin p_x + i \sin p_y}{\sqrt{\sin^2 p_x + \sin^2 p_y}} \quad (82)$$

The superscript 0 on the kets reminds us that these are going to be transformed to a more appropriate gauge later.

The angle  $\phi(\mathbf{p})$  is ill defined at  $\theta(\mathbf{p}) = 0, \pi$ . At  $\theta(\mathbf{p}) = 0$ , choice  $|\mathbf{p}\rangle_2$  is good because the component  $\sin \frac{\theta(\mathbf{p})}{2} e^{-i\phi(\mathbf{p})}$  vanishes. In a patch where  $\theta(\mathbf{p}) = \pi$ , the choice  $|\mathbf{p}\rangle_1$  is good. Figure 7 shows that there are four trouble spots:  $(0, 0)$  where the spinor is at the south pole  $\theta = \pi$ , and points  $(0, \pi)$ ,  $(\pi, \pi)$  and  $(\pi, 0)$  where it is at the north pole  $\theta = 0$ . We pick the BZ in the range  $[-\frac{\pi}{2}, \frac{3\pi}{2}]$  so that the trouble spots are not at the edges. Patch 1 is indicated by the solid right triangle and patch 2 is the rest.

The corresponding Berry connections are

$$\mathcal{A}_1^0(\mathbf{p}) = -\frac{1}{2}(1 + \cos \theta(\mathbf{p}))\nabla\phi \quad (83)$$

$$\mathcal{A}_2^0(\mathbf{p}) = \frac{1}{2}(1 - \cos \theta(\mathbf{p}))\nabla\phi \quad (84)$$

Once again the superscript 0 on the  $\mathcal{A}^0$ 's above signals that this is not yet the final gauge.

If we imagine the edges of the BZ parallel to  $\mathbf{e}_y$  glued together to form a cylinder and then the top and bottom sewn together to form the torus, this dark line will mark the boundary between the two regions. The difference between the two connections is  $-\nabla\phi$ , and the integral around the boundary of  $-\frac{1}{2\pi}\nabla\phi$  will yield  $\mathcal{C} = -1$ .

We now reach the final gauge  $\mathcal{A}_y = 0$  as follows. Let us define

$$\Lambda_1(p_x, p_y) = \int_{-\frac{1}{2}\pi}^{p_y} \mathcal{A}_{1y}^0(p_x, p_y') dp_y' \quad (85)$$

$$\Lambda_2(p_x, p_y) = \Lambda_1(p_x, \frac{\pi}{4} - \frac{p_x}{2}) + \int_{\frac{\pi}{4} - \frac{p_x}{2}}^{p_y} \mathcal{A}_{2y}^0(p_x, p_y') dp_y' \quad (86)$$

$$\chi(p_x) = \phi(p_x, \frac{\pi}{4} - \frac{p_x}{2}) \quad (87)$$

and the following final kets in the two patches

$$|\mathbf{p}\rangle_1 = e^{i\Lambda_1} |\mathbf{p}\rangle_1^0 \quad (88)$$

$$|\mathbf{p}\rangle_2 = e^{i\Lambda_2 + i\chi} |\mathbf{p}\rangle_2^0 \quad (89)$$

In this final gauge, not only is  $\mathcal{A}_y = 0$ , the two expressions above,  $|\mathbf{p}\rangle_1$  and  $|\mathbf{p}\rangle_2$ , merge seamlessly along the sloped line  $p_y = \frac{\pi}{4} - \frac{p_x}{2}$  separating the patches and on the vertical boundaries of the BZ, which may be glued to form a cylinder. However between the lines  $p_y = -\frac{\pi}{2}$  and  $p_y = \frac{3\pi}{2}$  there is a phase mismatch so that we cannot roll the cylindrical BZ to a torus without a discontinuity at the seam. This had to be so, for otherwise we would have a fully periodic Bloch function and  $\mathcal{C}$  would vanish by Stokes' Theorem<sup>39</sup>.

A salient feature of this gauge is that  $\rho_{\text{FCB}}(\mathbf{q})$  in Eq. 78 also has jumps in the sum over  $\mathbf{p}$  exactly where the  $\rho_{\text{GMP}}(\mathbf{q} + \mathbf{G})$ 's do, rendering this the optimal gauge for rapid convergence of the Fourier expansion.

Figure 8 gives a taste of how the Fourier expansion works at a generic value of  $\mathbf{q} = 3\mathbf{e}_x + 3\mathbf{e}_y$ . It compares, at fixed  $p_y = -\frac{\pi}{2} + 5$ , the imaginary part of the coefficient of  $d^\dagger([\mathbf{p} + \mathbf{q}])d(\mathbf{p})$  in  $\rho_{\text{FCB}}(\mathbf{q})$  to the approximation in which the Fourier sum over  $\mathbf{G}$  is truncated after 50 harmonics (from  $-25$  to  $25$ ) in the  $p_y$  direction and 20 in the  $p_x$  direction. Note that even though  $\mathbf{q}$  has components in both directions, the jump occurs only in the  $p_y$  direction due to the periodicity in the  $p_x$  direction.

Figure 9 shows the full landscape of the the real part of the coefficient of  $d^\dagger([\mathbf{p} + \mathbf{q}])d(\mathbf{p})$  in  $\rho_{\text{FCB}}(\mathbf{q})$  versus the approximation in which 50 harmonics (from  $-25$  to  $25$ ) are kept in the  $p_y$  direction and 20 in the  $p_x$  direction.

Having expressed everything in terms of  $\rho_{\text{GMP}}(\mathbf{q})$ , the the CF substitution and HF analysis can be carried out just as before and we do not discuss it further.

A central message of this work is that since in a prob-

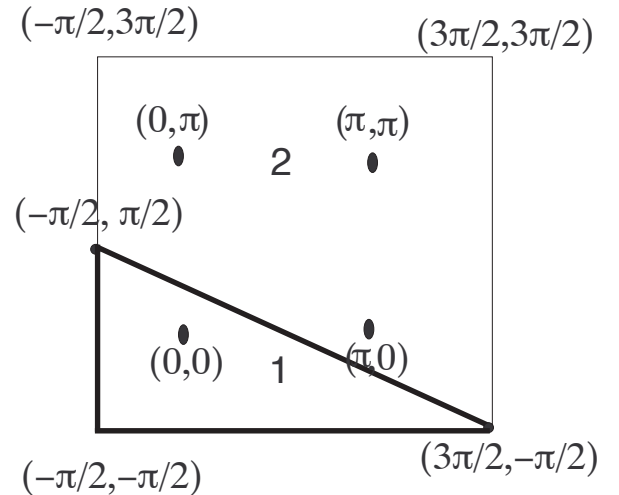


FIG. 7: In patch 1, we have the south pole at  $(0, 0)$  and spinor  $|\mathbf{p}\rangle_1$  is well defined while in patch 2, spinor  $|\mathbf{p}\rangle_2$  is well defined at the north pole reached at the points  $(0, \pi)$ ,  $(\pi, 0)$ ,  $(\pi, \pi)$ . The patches meet on the right triangle. In the final  $\mathcal{A}_y = 0$  gauge the wavefunction is seamless across the hypotenuse  $p_y = \frac{\pi}{4} - \frac{p_x}{2}$  and periodic in  $p_x$ . However the top and bottom edges differ by a phase and the Chern number is resident in that difference.

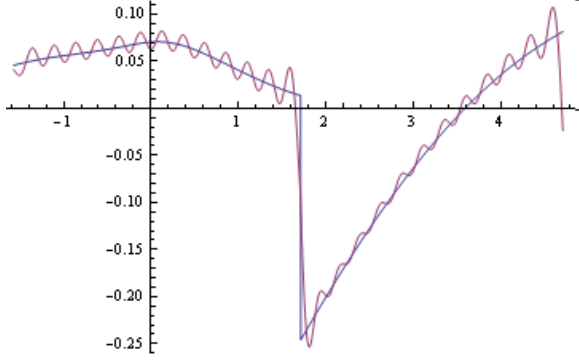


FIG. 8: Here we compare, at fixed  $p_x = -\frac{\pi}{2} + 5$ , the imaginary part of the coefficient of  $d^\dagger([\mathbf{p} + \mathbf{q}])d(\mathbf{p})$  in  $\rho_{\text{FCB}}(\mathbf{q})$  to the approximation in which the Fourier sum over  $\mathbf{G}$  is truncated after 50 harmonics in the  $p_y$  direction (from  $-25$  to  $25$ ) and 20 in the  $p_x$  direction.

lem with  $\mathcal{C} \neq 0$ , one cannot work with periodic Bloch functions, the expression for  $\rho_{\text{FCB}}(\mathbf{q})$  in the  $\mathcal{A}_y = 0$  gauge will necessarily have a jump beyond some  $p_y$  depending on  $q_y$  when we retract from a point  $\mathbf{p} + \mathbf{q}$  which lies outside the BZ to a point  $\mathbf{p}' = [\mathbf{p} + \mathbf{q}]$  within. The GMP density  $\rho_{\text{GMP}}(\mathbf{q})$ , has exactly such a jump and is the right basis to use. When the Chern band supports an FCI, CF coordinates are the natural variables in terms of which the system can be understood in the simplest way.

#### IV. THE CASE OF TRIVIAL BANDS

Let us ask if we have achieved “too much”. Consider a topologically trivial band with Chern number zero. Nothing prevents us from representing its projected density in terms of  $\rho_{\text{GMP}}(\mathbf{q} + \mathbf{G})$

$$\bar{\rho}(\mathbf{q}) = \sum_{\mathbf{G}} c(\mathbf{G}) \rho_{\text{GMP}}(\mathbf{q} + \mathbf{G}), \quad (90)$$

and carrying out the CF substitution. So, are there FCIs in topologically trivial bands?

This appears to be a subtle issue. On the face of it, since the Bloch spinor can now be globally defined as a periodic function in the BZ, so can  $\rho_{\text{FCB}}$ , and its expansion in terms of  $\rho_{\text{GMP}}$  which has a jump in the BZ seems ill fated. Although completeness assures us that with infinite number of terms we can do it, in order to give the expansion the best chance, we must first transform the spinor to the gauge  $\mathcal{A}_y = 0$ , just like the functions entering  $\rho_{\text{GMP}}$ . This makes  $\mathcal{A}_x(p_x, p_y + 2\pi) \neq \mathcal{A}_x(p_x, p_y)$  and causes the familiar jump.

The jump of this sort is inevitable if  $B(\mathbf{p})$  is non-constant, because in this gauge

$$\mathcal{A}_x(p_x, p_y) = - \int_{-\frac{\pi}{2}}^{p_y} \mathcal{B}(p_x, p'_y) dp'_y \quad (91)$$

and this integral need not vanish at any fixed  $p_x$ .

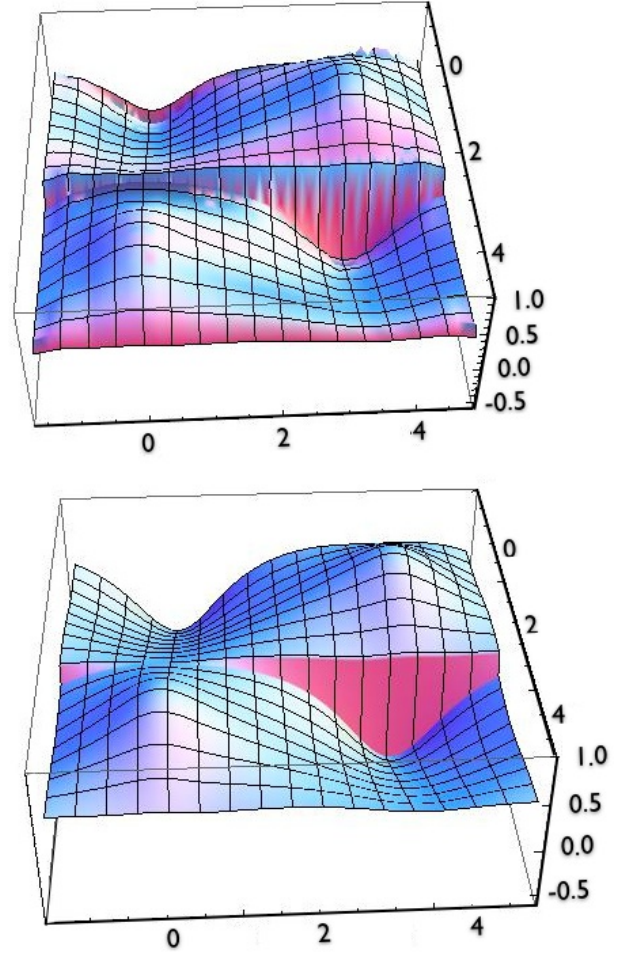


FIG. 9: The upper half shows the full landscape of the real part of the coefficient of  $d^\dagger([\mathbf{p} + \mathbf{q}])d(\mathbf{p})$  in  $\rho_{\text{FCB}}(\mathbf{q})$  in the approximation with 50 harmonics (from  $-25$  to  $+25$ ) in the  $p_y$  direction and 20 in the  $p_x$  direction. The lower one shows the actual values.

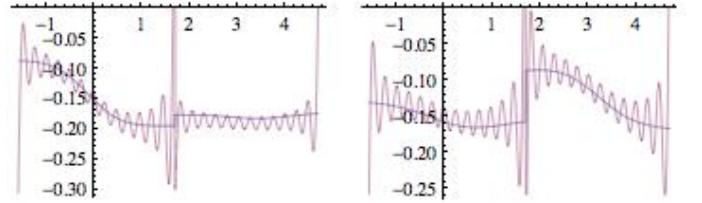


FIG. 10: Comparison, in the case with  $\mathcal{C} = 0$ , of imaginary parts of exact and approximate densities at  $p_x = -\frac{\pi}{2} + 1$  and  $p_x = -\frac{\pi}{2} + 6$  with the approximation truncated after 50 harmonics ( $+25$  to  $-25$ ) in the  $p_y$  direction

The Fourier expansion, while not so successful as in the case  $\mathcal{C} \neq 0$ , is still promising, as shown see Fig. 10 for two slices at  $p_x = -\frac{\pi}{2} + 1$  and  $p_x = -\frac{\pi}{2} + 6$ . The key feature is that the smaller the jump (i.e. the smaller the magnitude of  $\mathcal{B}(\mathbf{p})$ ) the more Fourier components it takes to approximate it to a given accuracy.

The bottom line is that, under certain conditions, even a band with  $\mathcal{C} = 0$  could exhibit FQHE under partial



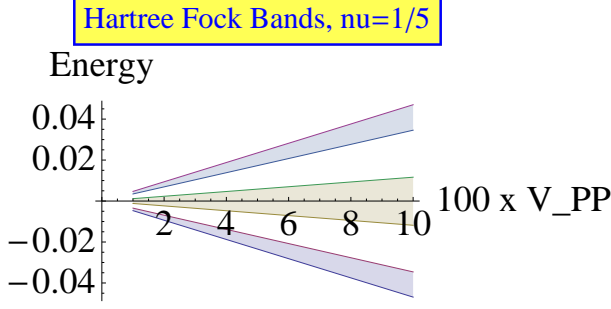


FIG. 11: The highest and lowest energies of the three sub-bands for the exotic fraction  $\frac{1}{5}$  as a function of the parameter  $V_{PP}$ . The bandwidths grows with the strength of the periodic potential but are still less than the sub-band gaps. The other parameters are  $V_{ee} = .1, \omega = 1$ .

filling, an issue we are actively pursuing.

So far we have been able to rule out the following completely trivial case: a band in which  $\mathcal{B}(\mathbf{p}) \equiv 0$  with no band dispersion. The energy is all potential and proportional to  $V_{ee}$ . Although an FCI state exists at  $\nu = \frac{1}{3}$ , its energy is always higher (by a factor of roughly 2) than the energy of the electronic Fermi liquid. Thus, in this case at least, FQHE does not appear to be favoured in the topologically trivial band.

## V. FRACTIONS WHERE $\nu \neq \sigma_{xy}$

In the presence of a periodic potential, the equality  $\nu = \sigma_{xy}$  is not mandatory, since Galilean invariance is explicitly broken. Exotic states whose very existence depends on an interplay of interactions and the lattice potential are possible<sup>34</sup>. There is suggestive numerical evidence for such states in a problem of lattice hard-core bosons in an external field<sup>35,36</sup>.

Since we have expressed the FCB Hamiltonian in CF language, it is natural for such states to be realized in FCBs under suitable conditions.

Consider a case with  $\nu = \frac{1}{5}$ . Each electron sees 5 flux quanta. Let us attach 2 (and not the usual 4) flux quanta to each electron to form CFs. Each CF sees 3 flux quanta and  $\nu_{CF} = \frac{1}{3}$ . In the continuum this partially filled CF-LLL is gapless, and thus not stable. However, as we will now show, such a state is generically gapped in the presence of a periodic potential. Since  $e^*/e = 3/5$ , the CF sees  $\frac{3}{5}$  flux quanta in the electronic unit cell. So we must take 5 times the electronic cell (say in the x-direction) to form a CF unit cell that encloses integer flux (3) and ensures that the CF translation operators  $T_x^5$  and  $T_y$  commute. In general if there are  $p/q$  quanta of effective flux per unit cell, each CF-LL will split into  $p$  sub-bands<sup>3</sup>. Thus, in our example each CF-LL will split into three sub-bands. If the lowest of these three sub-bands, when filled, is separated from the others by a gap, we obtain an FCI.

Our numerical work fully corroborates this picture. We work to linear order in the periodic potential  $V_{PP}$ ,

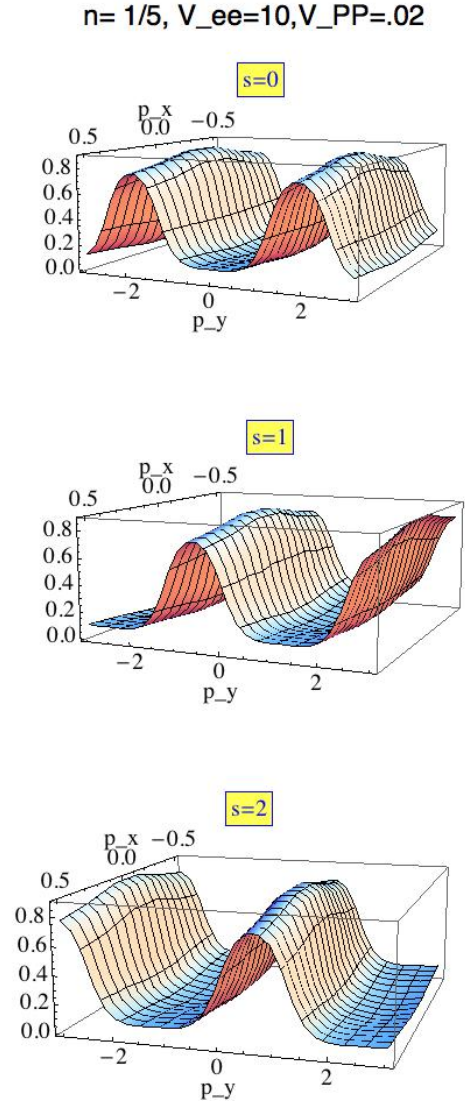


FIG. 12: From the top, the occupation numbers of the three CF-LLL sub-bands,  $s=0,1,2$ , for the exotic fraction  $\nu = \frac{1}{5}$ . The action of  $T_x^1, T_x^2, T_x^3, T_x^4$  is to change  $p_y$  by multiples of  $\frac{6\pi}{5}$  and change the sub-band index by 1 whenever  $p_y$  changes by  $2\pi$ . If the pictures of the three sub-bands are glued together in the order 0, 1, 2, we see 5 oscillations altogether.

and keep only the lowest CF-LL. Note that the treatment is not perturbative in the interaction strength. Fig. 11 shows the three sub-bands whose widths grow with the strength of the periodic potential while the gaps grow even faster. Figure 12 is very interesting. Once again  $T_x^1, T_x^2, T_x^3, T_x^4$  commute with  $H$  but not  $T_y$ . Each power of  $T_x$  changes  $p_y$  by  $\frac{6\pi}{5}$ . Starting with  $p_y = -\pi$  of the sub-band  $s = 0$ , if we act with these powers of  $T_x$ , we move to  $s = 1$  when the momentum change is  $> 2\pi$ , and to  $s = 2$  when the momentum change is  $> 4\pi$ . If the three pictures are glued end to end, we see 5 full oscillations. (Compare this to the  $\nu = \frac{1}{3}$  case where three periods occurred within the same CF-LL whereas here the 5 oscillations are spread over 3 sub-bands.)

What will be the Hall conductance of this state? We know from Kol and Read<sup>34</sup> that (in our convention where  $\mathcal{C} = -1$  for a filled LL)

$$\sigma_{xy} = \frac{\sigma_{\text{CF}}}{1 + 2\sigma_{\text{CF}}} \quad (92)$$

where  $\sigma_{\text{CF}}$ , the dimensionless CF Hall conductance (equal to minus its Chern number in our convention) of the filled sub-band could be any integer. (When a LL splits into sub-bands we only know that the sum of the Chern numbers of the sub-bands equals that of the original LL.) But no matter what this integer is, the possible values of  $\sigma_{xy} = \frac{1}{3}, \frac{2}{5}, \frac{3}{7}, \dots$  do not include  $\frac{1}{5}$ . The actual value happens to be  $\frac{2}{5}$  because  $\sigma_{\text{CF}} = 2$ .

## VI. SUMMARY AND OUTLOOK

We have demonstrated here that the Hamiltonian theory of the FQHE<sup>22</sup>, which was very useful in describing the FQHE in the continuum, is just as effective in describing fractionally filled Chern bands that exhibit FQH-like effects. This is surprising in view of the fact that since there is no external magnetic field in the FCB, ideas of flux attachment seem doomed from the outset. This is not an issue in our Hamiltonian theory which relies on an exact algebraic mapping that expresses the projected density of the Chern band  $\rho_{\text{FCB}}(\mathbf{q})$  in terms of CFs in two steps. First, we express  $\rho_{\text{FCB}}$  as a linear combination of operators  $\rho_{\text{GMP}}$  satisfying the magnetic translation algebra<sup>20</sup>. Second, we perform the CF substitution in  $\rho_{\text{GMP}}$  exactly as we did in the continuum theory<sup>22</sup>. These mappings of operator algebras can be carried out for arbitrary lattice models with no reference to Landau levels.

We have illustrated the power of the approach by solving two models. The first model is a  $\nu = \frac{1}{3}$  FCI and is adiabatically connected to the continuum Laughlin state at the same filling. The second is a more exotic,  $\nu = \frac{1}{5}$  FCI relying on the lattice potential for its very existence<sup>34</sup>. Its dimensionless Hall conductance is  $\frac{2}{5}$  and not  $\frac{1}{5}$  as would be expected in Galilean invariant state. In both cases we have computed the band structure of CFs in the Hartree-Fock approximation.

There are many interesting directions which we intend to pursue in future work. Collective excitations for fractionally filled Chern bands can be computed in a conserving approximation in our approach<sup>22,29,30</sup>, as can finite temperature effects<sup>22</sup>.

A specially interesting case is at  $\nu = \frac{1}{2}$  in a FCB. One expects an electronic Fermi liquid at weak coupling and an HLR-type CF-Fermi liquid at strong coupling. This transition, which we propose to study by our operator-based method, has already been explored in the parton formulation recently<sup>40</sup>.

Let us turn to quasiparticle excitations. In addition to Laughlin-type quasiparticles with fractional charge and statistics, the lattice allows us to consider excitations not conceivable in the continuum, such as those associated with lattice vacancies or dislocations<sup>41</sup>.

As stated in the introduction, fractionally filled 2D time-reversal invariant TIs<sup>5–11,13</sup> can be treated by labelling the pair of Chern bands making up the noninteracting TI (with equal and opposite Chern index) by a pseudospin index. There is no requirement of  $S_z$  conservation, and the interactions can produce states which can spontaneously break time-reversal, and/or states of the Kol-Read type. In fact, in a numerical diagonalization on a small system Neupert *et al*<sup>12</sup> find a state in a regime of parameters which has a filling of  $\frac{2}{3}$  but a degeneracy of 3 (rather than the degeneracy of  $3 \times 3 = 9$  one would expect for “independent”  $\nu = \frac{1}{3}$  for each pseudospin) on the torus, suggesting that it could be a Kol-Read<sup>34</sup> type state.

While finishing this manuscript we noticed the work of Grushin *et al*<sup>42</sup>, who have examined the conditions for the stability of the FCI.

We thank the NSF for grants DMR-0703992 and PHY-0970069 (GM), DMR-0103639 (RS), Yong-Baek Kim, Herb Fertig, Sid Parameswaran, and Nick Read for illuminating discussions and Anne-Frances Miller for help with the graphics. We are grateful to Shivaji Sondhi and Sid Parameswaran for urging us to confront the numerics. Finally, we are grateful to the Aspen Center for Physics (NSF 1066293) for its hospitality and facilitating our collaboration.

<sup>1</sup> F. D. M. Haldane, *Phys. Rev. Lett.*, **61**, 2015, (1988).

<sup>2</sup> G. E. Volovik, *Phys. Lett. A* **128**, 277 (1988); *Sov. Phys. JETP* **67**, 1804 (1988).

<sup>3</sup> D. J. Thouless, M. Kohomoto, M. P. Nightingale, and M. den Nijs, *Phys. Rev. Lett.*, **49**, 405, (1982).

<sup>4</sup> For reviews see, M. Z. Hasan and C. L. Kane, *Rev. Mod. Phys.* **82**, 3045 (2010); X.-L. Qi and S.-C. Zhang, arXiv:1008.2026, *Rev. Mod. Phys.* **83**, 1057 (2011); M. Koenig, S. Wiedmann, C. Bruene, A. Roth, H. Buhmann, L. W. Molenkamp, X.-L. Qi and S.-C. Zhang, *Science* **318**, 766 (2007).

<sup>5</sup> M. Levin and A. Stern *Phys. Rev. Lett.*, **103**, 196803. 2009.

<sup>6</sup> E. Tang, J. W. Mei and X.-G. Wen, *Phys. Rev. Lett.*, **106**, 236802, (2011).

<sup>7</sup> K. Sun, Z. Gu, H. Katsura and S. Das Sarma, *Phys. Rev. Lett.*, **106**, 236803, (2011).

<sup>8</sup> T. Neupert *et al*, *Phys. Rev. Lett.*, **106**, 236804, (2011).

<sup>9</sup> D. N. Sheng, Z. Gu, K. Sun, L. Sheng, arXiv:1102.2568, *Nature Communications* **2**, 389 (2011).

<sup>10</sup> N. Regnault and A. Bernevig, arXiv: 1105.4867, *Physical Review X* **1**, 021014 (2011); A. Bernevig and N. Regnault, *Phys. Rev. B* **85**, 075128 (2012).

<sup>11</sup> Y.-F. Wang, Z.-C. Gu, C.-D. Gong, and D. N. Sheng arXiv:1103.1686, *Phys. Rev. Lett.* **107**, 146803 (2011).

- <sup>12</sup> T. Neupert, L. Santos, S. Ryu, C. Chamon and C. Mudry, *Phys. Rev. B* **84**, 165107 (2011).
- <sup>13</sup> T. Liu, C. Repellin, A. Bernevig, and N. Regnault, arXiv:1206.2626[cond-mat]
- <sup>14</sup> X.-L. Qi, arXiv:1105.4298, (2011), *Phys. Rev. Lett.* **107**, 126803, (2011)
- <sup>15</sup> Yang-Le Wu, N. Regnault, B. Andrei Bernevig, arXiv:1206.5773 (2012).
- <sup>16</sup> J. Maciejko, X.-L. Qi, A. Karch, and S. C. Zhang (2010), *Phys. Rev. Lett.* **105**, 246809 (2010)
- <sup>17</sup> B. Swingle, M. Barkeshli, J. McGreevy, and T. Senthil, *Phys. Rev. B* **83**, 195139 (2011).
- <sup>18</sup> Y.-M. Lu and Y. Ran arXiv:1109.0226, *Phys. Rev. B* **85**, 165134 (2012).
- <sup>19</sup> S. A. Parameswaran, R. Roy and S. L. Sondhi, arXiv:1106.4025, *Phys. Rev. B* **85**, 241308 (R)(2012). See also M. Goerbig, *Eur. Phys. J.* **85(1)**, 15,(2012).
- <sup>20</sup> S. M. Girvin, A. H. MacDonald and P. M. Platzman, *Phys. Rev. B* **33**, 2481, (1986).
- <sup>21</sup> J. K. Jain, *Phys. Rev. Lett.*, **63**, 199, (1989).
- <sup>22</sup> G. Murthy and R. Shankar, Hamiltonian Theory of the fractional quantum Hall effect, cond-mat/0205326, *Rev. Mod. Phys.* **75**, 1101, (2003).
- <sup>23</sup> B. I. Halperin, P. A. Lee and N. Read, *Phys. Rev. B* **47**, 7312, (1993); V. Kalmeyer and S.-C. Zhang, *Phys. Rev. B* **46**, 9889, (1992).
- <sup>24</sup> Y.-H. Wu, J. K. Jain, K. Sun, arXiv:1207.4439.
- <sup>25</sup> J. M. Leinaas and J. Myrrheim, *Nuovo Cimento* **37B**, 1 (1977). F. Wilczek, *Phys. Rev. Lett.* **48**, 1144, (1982).
- <sup>26</sup> S. C. Zhang, H. Hansson and S. A. Kivelson, *Phys. Rev. Lett.*, **62**, 82, (1989).
- <sup>27</sup> A. Lopez and E. Fradkin, *Phys. Rev. B* **44**, 5246, (1991)
- <sup>28</sup> R. Shankar and G. Murthy, *Phys. Rev. Lett.*, **79**, 4437, (1997).
- <sup>29</sup> N. Read, *Phys. Rev. B* **58**, 16262 (1998).
- <sup>30</sup> V. Pasquier and F. D. M. Haldane, *Nucl. Phys. B* **516**, 719 (1998).
- <sup>31</sup> R. L. Laughlin, *Phys. Rev. Lett.*, **50**, 1395 (1983).
- <sup>32</sup> E. Fradkin, *Phys. Rev. B* **42**, 570 (1990); A. Lopez, A. Rojo, and E. Fradkin, *Phys. Rev. B* **49**, 10877 (1994).
- <sup>33</sup> D. Eliezer and G. W. Semenoff, *Annals of Physics* **217**, 66 (1991).
- <sup>34</sup> A. Kol and N. Read, *Phys. Rev. B* **48**, 8890 (1993).
- <sup>35</sup> A. S. Sorensen, E. Demler, and M. D. Lukin, *Phys. Rev. Lett.* **94**, 086803(2005).
- <sup>36</sup> G. Möller and N. R. Cooper, *Phys. Rev. Lett.* **103**, 105303 (2009).
- <sup>37</sup> D. Xiao, M. Chang, and Q. Niu, *Rev. Mod. Phys.* **82**, 1959, (2010).
- <sup>38</sup> G. Murthy and R. Shankar, arXiv:1108.5501, unpublished.
- <sup>39</sup> D. J. Thouless, *J. Phys. C* **17**, L325 (1984).
- <sup>40</sup> M. Barkeshli and J. McGreevy, arXiv:1206.6530[cond-mat].
- <sup>41</sup> M. Barkeshli and X.-L. Qi, arXiv:1112.3311.
- <sup>42</sup> A. G. Grushin, T. Neupert, C. Chamon, C. Mudry, arXiv:1207.4097.